Journal of Biomedical Optics 9(1), 230–238 (January/February 2004)

Monitoring neoadjuvant chemotherapy in breast cancer using quantitative diffuse optical spectroscopy: a case study

Dorota B. Jakubowski
Albert E. Cerussi
Frédéric Bevilacqua
Natasha Shah
University of California, Irvine
Beckman Laser Institute
Laser Microbeam and Medical Program
1002 Health Sciences Road East
Irvine, California 92612

David Hsiang
John Butler
University of California, Irvine Medical Center
Chao Family Comprehensive Cancer Center
101 The City Drive South
Orange, California 92868

Bruce J. Tromberg
University of California, Irvine
Beckman Laser Institute
Laser Microbeam and Medical Program
1002 Health Sciences Road East
Irvine, California 92612
E-mail: bjtrombe@uci.edu

Abstract. Presurgical chemotherapy is widely used in the treatment of locally advanced breast cancer. Monitoring the response to therapy can improve survival and reduce morbidity. We employ a noninvasive, near-infrared method based on diffuse optical spectroscopy (DOS) to quantitatively monitor tumor response to neoadjuvant chemotherapy. DOS was used to monitor tumor response in one patient with locally advanced breast cancer throughout the course of her therapy. Measurements were performed prior to doxorubicin-cyclophosphamide therapy and at several time points over the course of three treatment cycles (68 days). Our results show strong tumor to normal (T/N) tissue contrast in total hemoglobin concentration (T/N =2.4), water fraction (T/N=6.9), tissue hemoglobin oxygen saturation, S_tO_2 (T/N=0.9), and lipid fraction (T/N=0.7) prior to treatment. Over a 10-week period, the peak total hemoglobin and water dropped 56 and 67%, respectively. Lipid content nearly returned to baseline (T/N $=0.9$) while S_tO_2 exceeded pretreatment levels (T/N =1.5). Approximately half of the hemoglobin and water changes occurred within 5 days of treatment (26 and 37%, respectively). These data suggest that noninvasive, quantitative optical methods that characterize tumor physiology may be useful in assessing and optimizing individual response to neoadjuvant chemotherapy. [DOI: 10.1117/1.1629681]

Keywords: infrared spectroscopy; frequency-domain analysis; bio-optics; neoadjuvant therapy; breast cancer.

Paper 03011 received Feb. 10, 2003; revised manuscript received Jun. 27, 2003; accepted for publication Jul. 1, 2003.

1 Introduction

Presurgical, or neoadjuvant, chemotherapy has the advantage of decreasing tumor resection margins and allowing assessment of the effect of the chemotherapy drug regimen on the primary tumor. In stage III disease, reduced tumor margins will often change inoperable cases to operable. The prognosis for these patients is so improved that neoadjuvant chemotherapy has become well established for treating locally advanced breast cancer.[1] It is now also considered in stage I and II patients, when breast conservation is possible.[2–4]

In addition, neoadjuvant therapy permits evaluation of the primary tumor's response to a given drug combination. Without the primary tumor, the response of micrometastases to chemotherapy is not known. Many clinical trials are now using neoadjuvant therapy to answer questions regarding drug efficacy, dose, and frequency of administration.[5,6] Based on these studies, it is clear that at times it would be beneficial to change drug choices early in treatment in order to minimize morbidity and maximize patient survival.

Clinical palpation, although most widely used for gauging tumor response, is a relatively poor nonquantitative predictor of pathological response.[7,8] Results from the NSABP B-18 randomized control trial demonstrated that a significant increase in survival time was observed for a subpopulation of neoadjuvant chemotherapy patients who exhibited a complete histopathological response.[2] These patients had a 5-year survival rate of 87.2%. Regardless of clinical response, all other patients treated with neoadjuvant chemotherapy had virtually equivalent 5-year survival rates at or near 78%. This trial concluded that histopathological response to neoadjuvant chemotherapy is an independent prognostic factor in survival, a result suggested by earlier studies.[1,9] Unfortunately, complete pathological response is not often accomplished. Carlson's literature review in 1999 found the complete pathological response in locally advanced breast cancer to range between 4 and 33% for anthracycline-based therapy.[1] If any improvements in patient outcome are to be made, the results of imaging methods must correlate very closely with tumor pathology.

Several alternative methods for increasing the reliability of tumor assessment have been proposed. Mammography has had favorable results when it is coupled with physical examination, particularly in breasts with low mammographic density.[8] The presence of fibrotic tissue,[8] high mammographic density,[10] remaining microcalcifications,[10,8] or ill-defined tumors,[7,11] however, makes response more difficult to assess,

1083-3668/2004/$15.00

and several studies have found inadequate correlation with pathology or prognosis.[12,7,9,10,13]

Ultrasound may be more accurate than mammography in evaluating true tumor size;[14] however it has limited tumor versus normal contrast.[10] Color Doppler ultrasound may reveal changes in tumor vascularity before alterations in clinical dimensions are detected,[15] but the method is highly operator dependent.[16]

Evaluation of tumor size using magnetic resonance imaging (MRI) correlates better to pathology than mammography and has successfully located residual disease.[17] Especially promising results have been seen with dynamic contrast-enhanced methods.[18–20] However, MRI is costly and requires exogenous contrast agents. Cost becomes especially prohibitive if the tumor is repetitively monitored throughout treatment, as for assessment of drug susceptibility (early) or establishment of treatment end points (late).

Other methods used for monitoring tumor response include technetium 99m-MIBI scintigraphy,[21,22] and [^{18}F] FDG position emission tomography (PET).[23–25] Despite a relatively low resolution compared with MRI, tumor changes have been shown as early as 8 days after treatment.[26] Like MRI, scintigraphy requires the administration of exogenous agents.

Optical methods are intrinsically sensitive to blood, water, and lipid, the main chromophores of breast tissue. Thus they measure tissue composition, information that is qualitatively different but complementary to that of the structural images provided by mammography and ultrasound. In addition, optical methods are able to quantify oxygenated hemoglobin (HbOx) and deoxygenated hemoglobin (Hb). Thus hemoglobin oxygen saturation levels determined by this method are direct and absolute, albeit at low resolution.

A strong advantage of optical probes is that they can be portable, rapid, and noninvasive. They are effective without (or in conjunction with) exogenous contrast agents.[27,28] Because of this, quantitative measurements can be performed on almost all patients. However, optical methods have not been widely tested clinically. Mainly this is due to the youth of the field, which relies on relatively recent technology and computation-intensive fitting methods. Optical methods are currently being evaluated for use in breast cancer detection and monitoring.[29,30] The most significant limitation at this early date is spatial resolution and sensitivity to small lesions.

We have developed a broadband laser breast scanner (LBS) that combines steady-state (SS) and frequency-domain (FD) diffuse optical spectroscopy (DOS) in a single instrument.[31] The LBS employs the principles of photon diffusion to quantitatively measure absorption and scattering properties of tissue in the near-infrared spectral region (650 to 1000 nm). As mentioned previously, deoxygenated hemoglobin, oxygenated hemoglobin, lipid, and water are the main absorbers, or chromophores, in breast tissue at these wavelengths.[32] These components are by definition directly affected in cancer-related changes such as angiogenesis, cellular proliferation, hypoxia, and extracellular matrix degradation.[32,33] LBS measurements have been used to quantitatively measure these components in order to reveal age- and hormone-related changes in normal breast, as well as to characterize tumors.[31–35] Similar results have been obtained by others using photon migration spectroscopy and imaging.[28]

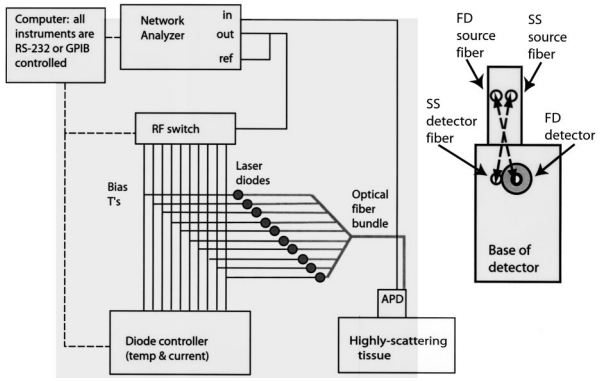

Fig. 1 Instrument setup: The frequency-domain (FD) system consists of 7 to 10 laser diodes that are intensity modulated using a network analyzer. The steady state (SS) spectroscopy system (not shown) consists of a high-intensity white-light source and spectrometer. The detector configuration is on the right. APD, avalanche photodiode; RF, radio frequency.

In this work we employed a portable, noninvasive DOS system to monitor a postmenopausal woman undergoing neoadjuvant chemotherapy for locally advanced breast cancer. Our goal was to assess the sensitivity of this method to changing tumor physiology throughout therapy. We followed this patient for three cycles of doxorubicin-cyclophosphamide (AC) and found excellent sensitivity to tumor response. AC-induced changes in all four major biochemical components as well as functional indices of oxygen utilization were clearly evident as early as the first week of therapy. All tumor levels approached control values by the end of the 68-day measurement period. Residual abnormalities recorded at the tumor site on the final measurement day (day 68) matched postsurgical histopathology findings. These results establish DOS sensitivity to biochemical changes in breast tissue that accompany tumor growth and response to therapy. Because the LBS is a portable, bedside device, this approach may become feasible for quantitatively monitoring tumor response, particularly where rapid or frequent measurements are required.

2 Materials and Methods

2.1 *Instrumentation*

The combination of frequency-domain and steady-state reflectance methods (SSFD) permits acquisition of broadband near-infrared absorption spectra. The broadband LBS instrument and method were previously validated on tissue phantoms and demonstrated on normal breast tissue.[31] The principles of operation have been well characterized and are only summarized here. Frequency-domain instrumentation,[36] the underlying theory of optical diffusion,[37] FD methods,[38,39] and steady-state methods[40] have all been extensively investigated and described.

The SSFD instrument and probe design are illustrated in Fig. 1. Measurements are recorded in reflectance (i.e., backscattering) geometry. Three optical fibers (SS and FD source, SS detector) and an avalanche photodiode (APD) (FD detector) are embedded in the face of the probe as shown. In this configuration, the SS and the FD measurement paths cross one another, allowing the SS and FD sources to probe ap-

proximately the same volume of tissue. In this set of experiments, the source–detector separation for both SS and FD measurements was 26 mm.

The FD component of the system uses ten diode lasers coupled to 400-μm step-index optical fibers formed into a single bundle. Laser wavelengths are 660, 685, 786, 809, 822, 852, 898, 911, 946, and 973 nm. Direct current is applied sequentially to each diode, followed by a 50 to 1000-MHz radio frequency (rf)-swept pulse from a network analyzer. This produces amplitude-modulated light that, when launched into the tissue, propagates with a frequency-dependent phase velocity as diffuse photon density waves.[41] Changes in photon density wave phase and amplitude are detected by the avalanche photodiode in the hand-held probe. The system is calibrated using tissue phantoms with known optical properties at the beginning of each 1 to 2-h measurement session. The SS component of the system consists of a high-intensity tungsten-halogen source launched onto a 3-mm fiber optic bundle. Diffuse reflectance is measured using a 1-mm fiber coupled to a spectrometer (USB2000, OceanOptics, Inc.) that is capable of measuring the reflectance spectra between 600 and 1000 nm. The SS system is calibrated at each measurement session using an integrating sphere with a nearly flat spectral response over the wavelength region of interest. A typical broadband measurement, consisting of both SS and FD components, is acquired in 30 to 45 s.

Both datasets are analyzed with in-house software developed in MATLAB (version 6.0.0.88, The MathWorks, Inc). Optical transport theory is used to extract the tissue scattering and absorption properties, resulting in quantitative measurements of the tissue concentration of oxygenated and deoxygenated hemoglobin, water, and lipid. The exact algorithm used is detailed in Bevilaqua et al.[29] The tissue concentration of deoxygenated and oxygenated hemoglobin can also be recombined in terms of total hemoglobin ($[Hb_{tot}]=[Hb]+[HbOx]$) and tissue hemoglobin oxygen saturation ($S_tO_2=100\times[HbOx]/[Hb_{tot}]$). These parameters are particularly important for comparing results with known medical standards, such as blood hematocrit (the percent of whole blood occupied by red blood cells) and blood hemoglobin oxygen saturation.

2.2 *Patient*

A 54-year-old postmenopausal Caucasian female with a previous right mastectomy underwent neoadjuvant therapy for cancer of the left breast. The patient was informed and consented under University of California protocol 95-563. The tumor was palpable in the lower inner quadrant and diagnosed as an adenocarcinoma by fine needle aspiration. Two weeks before treatment, the mammogram revealed a 2.3×2.5-cm mass with microcalcifications (Fig. 2). Ultrasound showed a hypoechoic mass measuring 2.4×2.5×2.2 cm (Fig. 3). The patient began three cycles spaced 3 weeks apart of a doxorubicin-cyclophosphamide drug combination. The tumor was judged nonpalpable at the conclusion of the three cycles, and the patient was scheduled for surgery. Surgical pathology revealed a stellate fibrotic lesion measuring 2.0×1.0×1.0 cm at the location of the treated tumor. Microscopy reported a 5-mm residual tumor within the fibrosis. The tumor was approximately a 10% intraductal carcinoma of high nuclear grade. The remainder was a moderately differentiated invasive ductal carcinoma. No necrosis was present.

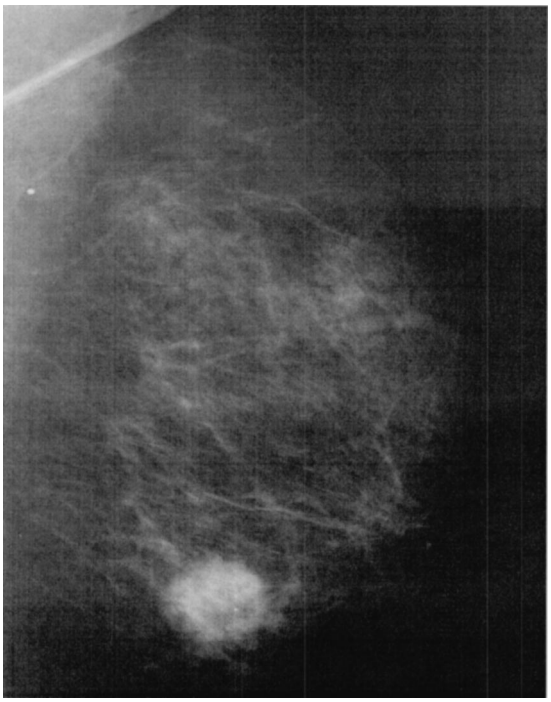

Fig. 2 Mammogram of a 54-year-old woman with an adenocarcinoma of the breast. This mediolateral oblique view shows a 2.3×2.5-cm mass with microcalcifications in the left lower inner quadrant.

2.3 *Measurements*

A series of scans was performed spanning 68 days and three treatment cycles. Measurements were recorded on a total of 12 different days and data were acquired over two different

Fig. 3 Ultrasound of a 54-year-old woman with an adenocarcinoma of the breast. Ultrasound shows a hypoechoic mass measuring 2.4×2.5×2.2 cm in the left lower inner quadrant.

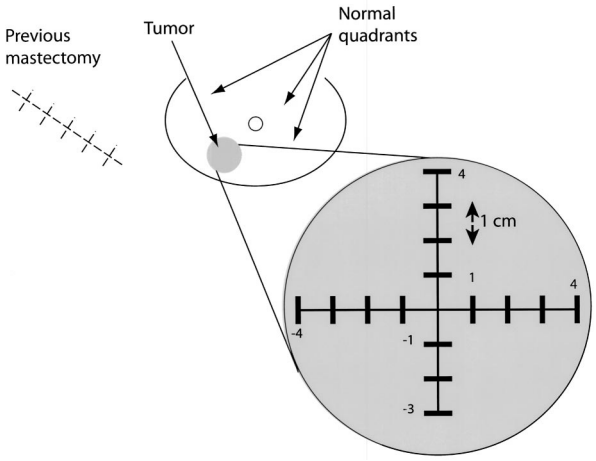

Fig. 4 Measurement configuration. Two linear scans were done in mutually perpendicular directions: along the cranial-caudal (sagittal) axis and along the medial-lateral (transverse) axis. The heavy lines are the source–detector paths for each of seventeen positions along the axes, placed at 1-cm increments (those at origin are not shown).

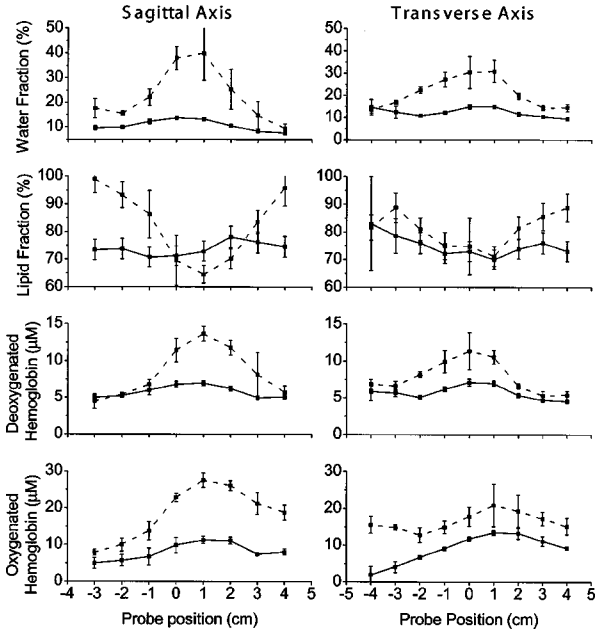

Fig. 5 Pretreatment (dashed lines) and post-treatment (solid lines) linear scans along both sagittal and transverse axes. At the tumor site, the water volume fraction and both components of hemoglobin increase, whereas the lipid volume fraction decreases. Although the tumor was not palpable after treatment, a residual perturbation was present in all parameters at the conclusion of the study.

axes. The measurement geometry is illustrated in Fig. 4. In all cases the patient was positioned supine at 30 deg elevation. One complete scan consisted of seventeen measurements taken over the tumor. These measurements consisted of two linear scans taken along perpendicular axes, medial-lateral (transverse) and cranial-caudal (sagittal) at 1-cm intervals, so that the total region sampled was 8 cm (nine measurements) along the transverse axis and 7 cm (eight measurements) along the sagittal axis. In each measurement the source and detector of the probe were positioned to bracket the axis, sampling a cross-section through the axis. Care was used to maintain probe contact with the skin while at the same time minimizing compression of the breast.

At any one location, a complete measurement consisted of a continuous white-light spectrum spanning the 650 to 1000-nm wavelength region and ten laser diode datasets from within the same region. Each of the latter consisted of an averaged scan of three phase and amplitude recordings at 401 intermediate modulation frequencies in the 50- and 700-MHz range. The dataset was then fit to a set of diffusion theory equations and principal component spectra[42,35] to obtain lipid, water, and deoxygenated and oxygenated hemoglobin concentrations at that location.

To obtain measurement reproducibility, a complete linear scan was typically repeated twice during any given measurement session. This resulted in a total of four linear scans (thirty-four cross-sectional measurements) per measurement session, plus the control measurements described later. The errors listed are the variation between the two scans. When maxima and minima are shown, errors are the variation between the maxima and minima of the two different scans. All errors found to be less than 5% by this method were set to 5%. In our experience, this is our average error, which is due to probe position and tissue coupling variability. In comparison, errors that are due to instrumentation and pressure changes within the tissue are minimal.

Given the large variability in normal breast physiology,[35] the most appropriate control for a breast tumor is the normal breast tissue of the same woman measured, if appropriate, at the same time point in the menstrual cycle, and ideally in the corresponding contralateral quadrant. In the patient studies, a previous mastectomy on the contralateral side prevented us from obtaining control measurements at the analogous tumor location. Instead, control measurements were taken on other quadrants of the same breast. The quadrants used as controls were clear of disease, as determined by mammography and postoperative pathology. The abdomen was used as a systemic control.

In the first cycle, optical scans were obtained immediately prior to chemotherapy treatment (day 0) and daily (days 3, 4, 5, 6, 7) during the following week. In the second cycle, optical scans were taken immediately prior to chemotherapy treatment and every other day (days 21, 24, 26, 28) during the following week. No scans were scheduled during the third cycle because we did not believe the patient was well enough to travel to the clinic. The final two scans were obtained on separate days approximately 3.5 weeks after the final chemotherapy treatment date and 13 days prior to surgery. Although scans were obtained on 12 separate days, data from 4 days could not be analyzed because of instrument-related errors. These were due either to problems with spectrometer operation (3 days) or system calibration (1 day).

3 Results

Figure 5 displays the pretreatment and post-treatment line scans over the tumor for all four chromophores. Both the sagittal and the transverse axes are shown. With the exception of the 4 and −4-cm positions, each probe position is an av-

Table 1 Tumor to control ratios for chromophores measured along the sagittal and transverse axes.

	Sagittal Axis		Transverse Axis	
Chromophore[a]	Pretreatment	Post-treatment	Pretreatment	Post-treatment
Lipid	0.66	0.87	0.72	0.89
Water	6.93	2.09	5.28	2.59
Hb	2.66	1.10	2.27	1.12
HbOx	2.31	2.02	1.62	2.60
S_tO_2	0.95	1.35	0.89	1.49
Hb+HbOx	2.42	1.51	1.82	1.77

[a] Hb, deoxygenated hemoglobin; HbOx, oxygenated hemoglobin; S_tO_2, tissue hemoglobin oxygen saturation.

erage of two repeat measurements where the probe was removed from the patient and replaced in the same position.

The pretreatment tumor perturbation against background is clearly visible in all chromophores along both axes. These scans were obtained on the day of the first chemotherapy treatment, just prior to administration (day 0). The sagittal scan most closely approaches the midpoint of the tumor. Along this axis, the water volume fraction peaks at 40 $\pm$11% and drops to 9$\pm$2% at the lowest edge location. The corresponding fraction of lipid volume dips by approximately one third at the tumor center. Compared to edge values, deoxygenated and oxygenated hemoglobin components also peak by a maximum of roughly 3 and 3.5 times over the tumor.

As Fig. 5 illustrates, SSFD values over the tumor undergo significant changes at the conclusion of the 10-week measurement period. All parameters approach baseline. However, all parameters have lingering changes over the tumor location. At the conclusion of treatment, the lump was no longer palpable, although a 5-mm residual tumor was noted in postsurgical pathology.

Table 1 provides the resulting tumor to control ratios for the pretreatment and post-treatment (presurgical) scans shown in Fig. 5. Measurements from the left upper outer quadrant are used as control values for these ratios. Edge values of the linear scans from Fig. 5 are not used because these values do not necessarily normalize, and therefore are not entirely outside the boundary of the tumor. In addition, the size of the tumor changes during treatment, so that these edge values are not expected to stay constant.

The most significant contrast is seen in the water volume fraction. On the sagittal axis, the pretreatment water volume fraction at its peak is 6.9 times higher than that of control breast tissue. After treatment, this value drops to 2.1. With the exception of the tissue hemoglobin oxygen saturation, S_tO_2, all other parameters also approach unity over the course of treatment.

Unless otherwise noted, the remaining results are presented from the sagittal axis. Data along the transverse axis follow similar, if diminished, trends. Figure 6 displays the

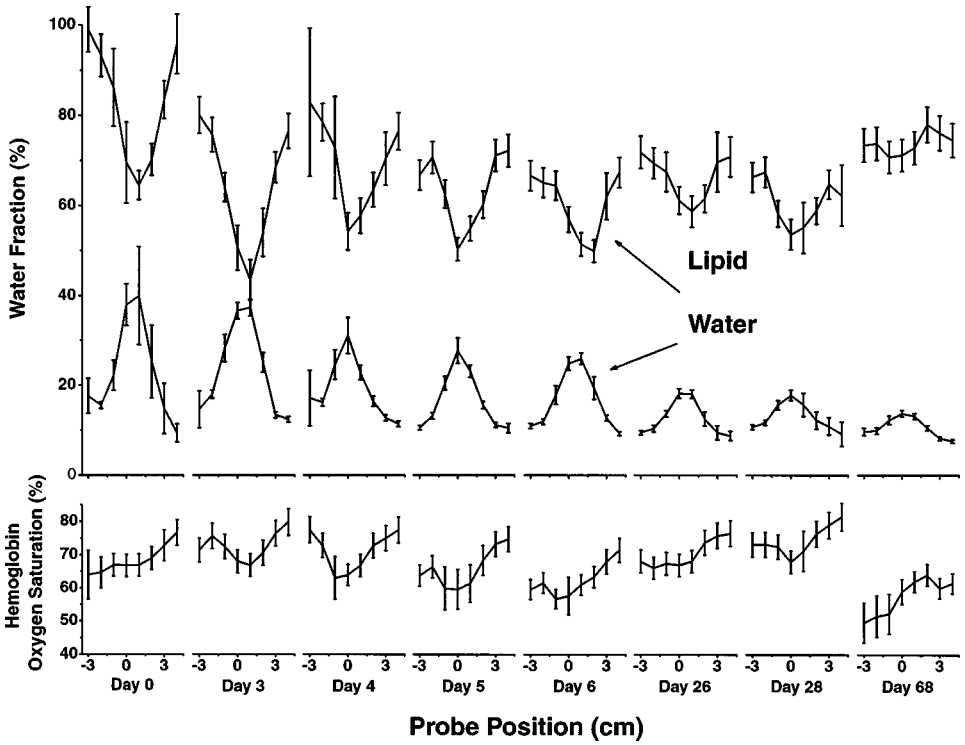

Fig. 6 All linear scans along the sagittal axis of water volume fraction, lipid volume fraction, and hemoglobin oxygen saturation done over the course of the 10-week study. The perturbations caused by the tumor in the water and lipid volume fraction have a correlating location and amplitude.

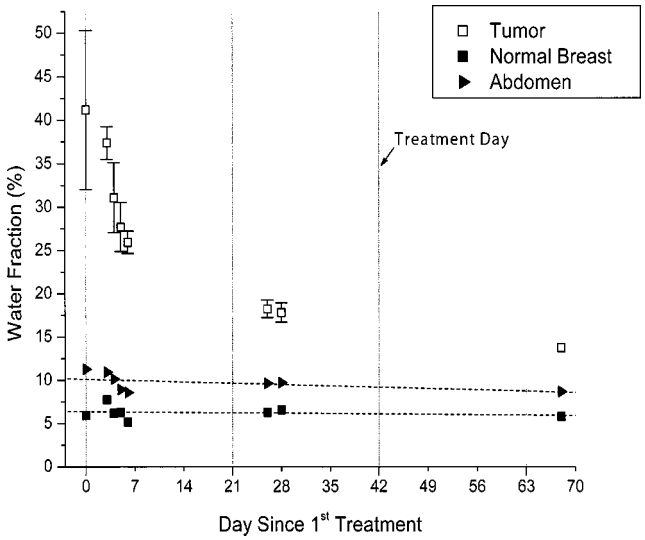

Fig. 7 Water volume fraction maxima located over the tumor as a function of the day in the study, along with control values from the abdomen and breast. Values over the tumor fall rapidly, whereas control tissues maintain constant levels. Error bars within points have been removed.

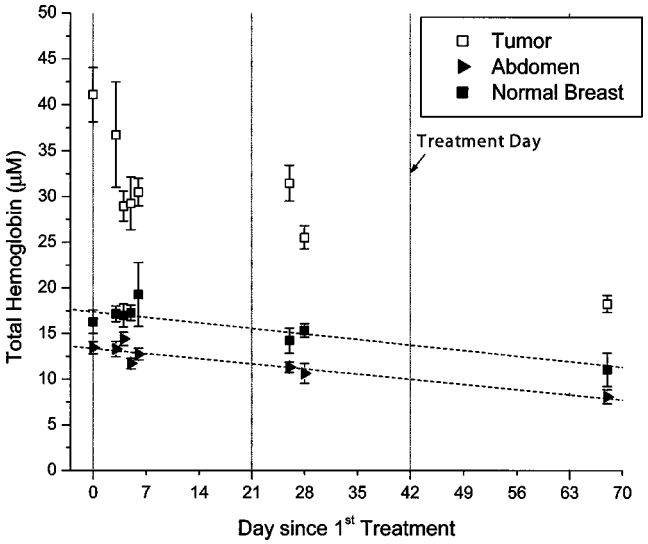

Fig. 8 Total hemoglobin maxima located over the tumor as a function of the day in the study, along with control values from the abdomen and left upper outer quadrant of the breast. Although total hemoglobin values at the tumor site consistently fall, control values also decrease.

successive linear scans of lipid volume fraction, water volume fraction, and S_tO_2 over the 10-week course of therapy. Values for the water volume fraction peak and those for the lipid volume fraction dip to a similar degree over the tumor for all days. The tumor perturbation diminishes consistently throughout the course of the study. This is especially striking in the water volume fraction. S_tO_2 typically dips at the tumor location, except for a modest peak that develops by day 68, well after the conclusion of chemotherapy and just prior to surgery.

The full course of the peak value for the water volume fraction is plotted over time in Fig. 7, along with control measurement values acquired on the abdomen and the left upper outer quadrant of the breast. As noted previously, values over the tumor steadily decrease, approaching the values for the left upper outer quadrant. In this figure it is also apparent that the greatest changes occur within the first week. In 10 weeks, the maximum water volume fraction drops 67% from its original value ($41\pm9\%$ to $13.7\pm0.7\%$), whereas control measurements from the left upper outer quadrant do not change significantly ($5.9\pm0.3\%$ to $5.8\pm0.3\%$). The drop in water volume fraction is appreciable as early as a few days after the first treatment, changing by 37% (to $26\pm1\%$) within the first week. It is interesting that control abdomen and left upper outer breast values also drop by about 20 to 25% during this early period, suggesting the possibility of reactive systemic changes immediately following chemotherapy.

Similar to the trend seen in the water volume fraction, total hemoglobin concentrations over the tumor drop substantially during therapy. Figure 8 shows the total hemoglobin maxima plotted for the 10-week period. From the first to the last measurement, total hemoglobin drops from $41\pm3\ \mu$M to $18.2\pm0.9\ \mu$M, a 56% decrease. Again, approximately half of the drop occurs within the first week (26%; to $30\pm2\ \mu$M). However, both controls also gradually decrease over 10 weeks. From the first to the last measurement, total hemoglobin measured on the left upper outer breast quadrant drops 32% (16 ± 1 to $11\pm2\ \mu$M). A 40% decrease is observed in the abdominal control (13.4 ± 0.7 to $8.1\pm0.8\ \mu$M). This downward trend in both control locations implies a systemic drop in hemoglobin. Blood hematocrit levels obtained from routine blood work were observed to steadily decrease from a high of 36.7% at the initiation of treatment to a final low of 30.7% at the conclusion of treatment, a 16% drop.

When the total hemoglobin is divided into oxygenated and deoxygenated components, it can be seen that the downward trend is due mainly to the oxygenated component. Figure 9 shows both oxy- and deoxyhemoglobin levels in control tissue (abdomen and control breast tissue) over the 10-week period. Control breast measurements of deoxygenated hemoglobin vary minimally over the entire treatment course (5.1 ± 0.8 to

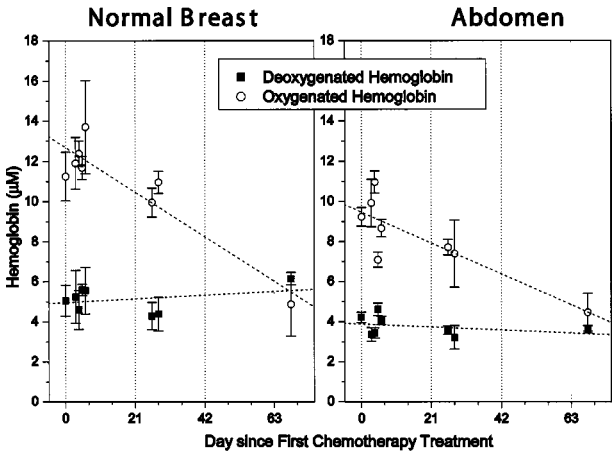

Fig. 9 Deoxygenated and oxygenated hemoglobin values over the treatment course. The left panel represents measurements on normal breast tissue and the right represents abdominal tissue. In both control sites, oxygenated hemoglobin drops over the course of the study whereas deoxygenated hemoglobin remains fairly constant.

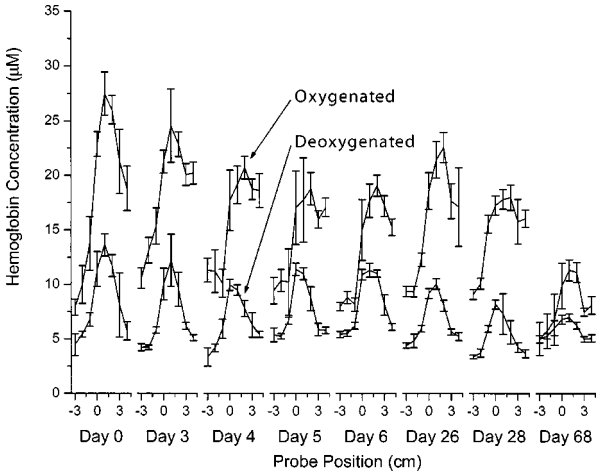

Fig. 10 All linear scans (sagittal axis) of deoxygenated hemoglobin and oxygenated hemoglobin over the treatment course. The baseline of the oxygenated hemoglobin shifts downward; however, that of the deoxygenated hemoglobin stays fairly constant. This is consistent with the trends observed in the control tissues.

$6.1 \pm 0.3\ \mu$M; within errors) compared with the relatively large change in oxygenated hemoglobin (11 ± 1 to $5 \pm 2\ \mu$M; 57% drop). The same trend is present in control abdominal measurements.

Figure 10 displays details of oxygenated and deoxygenated hemoglobin linear scans over the tumor area for the full 10-week course. The trends are similar to those already noted in that the oxygenated hemoglobin component has a downward trend in its baseline that is not present in the deoxygenated component. Deoxygenated hemoglobin peak values decrease 50% from the first to the last measurement ($14 \pm 1\ \mu$M to $7.0 \pm 0.4\ \mu$M). In the first week, they drop 17% (to $11.3 \pm 0.6\ \mu$M), again with negligible changes for control sites (Fig. 9).

4 Discussion

Neoadjuvant chemotherapy is the indicated treatment of locally advanced breast cancer, and its breast-conserving properties have caused it to come under consideration in the management of stage I and stage II disease.[2–4] A number of methods have been used to monitor changes in the primary tumor during treatment, with varying success. Near-infrared diffuse optical spectroscopy has the advantage of being portable, free of contrast agents, fast, and inexpensive. However, the technology on which this method is based is relatively new, and few studies have been conducted in clinical settings that establish the sensitivity of DOS to tumor physiology. This pilot study is specifically meant to determine the feasibility of using diffuse optical spectroscopy for monitoring tumor changes throughout the treatment cycle, and to evaluate whether DOS has potential for predicting early therapeutic response.

In general, the behavior of all parameters measured at the tumor is consistent with expected changes in tumor physiology. All parameters have a maximum or minimum contrast in the tumor location that eventually diminishes over the course of the treatment, with the steepest changes occurring in the first week of treatment.

It is apparent from the spatial profiles on any given day, however, that certain parameters do not peak at the same physical location. For instance, the dip in tissue hemoglobin oxygen saturation on the transverse axis is at the probe position -1, whereas all other parameters have extrema at $+1$. Although this may be due to inherent measurement error, it is most likely due in part to tumor physiology. Tumor heterogeneity, with significantly different fractions of blood, water, and lipid, can result in unique spatial variations for all examined constituents. This is especially true of larger tumors, in which areas of necrosis are more likely.

We were particularly concerned with how well we could consistently return to the same location on the tumor from day to day. In the first week, we were able to return to calibration lines drawn on the skin. At later time points, having to relocate the tumor center by palpation certainly increased our errors. However, the presence of a water and hemoglobin peak in the optical measurements reassured us that we were capable of identifying the tumor core despite the fact that it was not clinically palpable at later time points in this study. A full 2-D grid of the area, instead of two perpendicular scans, would have allowed us to limit sampling errors further.

Scans over the tumor are consistent with a highly vascularized cellular mass surrounded by mostly fatty tissue. The water content measured over the tumor increases, as expected, for a cellular mass located in a lipid-rich background. In addition, elevated water content may be an indication of local edema or necrosis. The decrease in the lipid volume fraction and the decrease in water content are co-localized throughout the 10-week treatment (Fig. 6). This results in tumor and control water to lipid ratios that drop from ~ 10.5 to ~ 2.4 after three cycles of chemotherapy (data may be extrapolated from Table 1). This 4.4-fold reduction in contrast is in excellent agreement with previous findings from magnetic resonance spectroscopy that tumor and control water to lipid ratios change from ~ 16.7 to ~ 3.9, a factor of approximately 4.3, over the course of three chemotherapy cycles.[43]

High blood volume at the tumor site, as indicated by total hemoglobin, is compatible with the increase in blood vessel density frequently noted in breast tumors. However, control measurements on both the abdomen and breast show that total hemoglobin values also track hematocrit measurements obtained by *ex vivo* blood analysis. Thus, total hemoglobin alone is insufficiently sensitive to alterations in tumor vasculature since $[Hb_{tot}]$ is convolved with hematocrit fluctuations (Fig. 8). It is important to note that deoxygenated hemoglobin control measurements appear to be independent of hematocrit changes (Fig. 9). The deoxygenated hemoglobin in control tissues is produced by oxygen demand in local tissue beds. This demand should be unaffected by small changes in hematocrit. In contrast, chemotherapy-induced depletion of erythrocytes primarily affects the supply of oxygenated hemoglobin, which accounts for the HbOx drop in control tissue. As a result, deoxygenated hemoglobin levels are not influenced by modest fluctuations in hematocrit, and levels over the tumor are directly related to local tumor changes. Such alterations can still include a variety of effects, including physical contraction of a tumor and changes in oxygen demand in the region.

Over the course of the study, complementary changes were seen in water, lipid, and oxy- and deoxyhemoglobin. The perturbation made by the tumor compared to background control tissue decreases over time. These alterations are detectable and, in some cases, quite significant within the first week. In all measurements, trends are in the direction of the control baseline values obtained from the upper outer quadrant. This trend is consistent with the interpretation that the tumor is contracting over the course of treatment. In particular, water and all hemoglobin components decrease while lipid increases. The decrease in hemoglobin over the tumor is compatible with studies showing a reduction in angiogenesis in tumors after neoadjuvant therapy.[44] The rate of change in the deoxygenated hemoglobin peak is not as accelerated as that in total or oxygenated hemoglobin, presumably because the latter also reflects a global hematocrit drop.

In pretreatment measurements, tissue hemoglobin oxygen saturationlevels (S_tO_2) at the tumor are lower than those in surrounding normal areas, suggesting increased local metabolic activity or blood pooling. S_tO_2 values are considerably lower than conventional measurements of arterial hemoglobin oxygen saturation (i.e., pulse oximetry or S_aO_2) because near-infrared diffuse optical spectroscopy samples a mixture of arterial and venous microvasculature, and hence is sensitive to local metabolism. Tissue hemoglobin oxygen saturationmeasurements are particularly interesting because S_tO_2 values shift from a dip to a mild peak over the 10 week course of treatment. The shift indicates that the area has changed from one of relatively high metabolic demand to low metabolic demand, compared with surrounding areas. This is again consistent with pathology, which reports large regions of the tumor replaced by fibrotic tissue.

In the final presurgical measurement (day 68), a residual peak is present in the tumor water and hemoglobin. A residual dip is seen in lipid. This is most likely a consequence of our combined sensitivity to the small active tumor site and the surrounding fibrotic tissue (5 mm and 2 cm from pathology, respectively). The persistent increase in total hemoglobin at the tumor most likely reflects the residual vascularized tumor. Since a high vascular index after neoadjuvant therapy has been implicated in the 5-year risk of recurrence in node-positive invasive breast cancer,[45] this has possible consequences with regard to prognosis. The ability to quickly and noninvasively determine tumor blood volume, saturation, water, and lipid signatures will ultimately provide useful insight into the extent of viable, necrotic, and normal tissue types, since each zone is expected to have characteristic signatures.

In summary, we have found that quantitative, near-infrared diffuse optical spectroscopy is capable of distinguishing between tumor and surrounding breast tissue in a clinical subject. We have applied this method to monitoring neoadjuvant chemotherapy response and have observed significant changes in as little as a few days after the first course of treatment. Reductions in tumor water content are especially dramatic, although significant alterations are recorded in all parameters, including total hemoglobin, tissue hemoglobin oxygen saturation, and lipid content. These variations were measured with a portable, bedside, noninvasive hand-held probe. As tumor monitoring becomes more feasible at the bedside, treatment may be modified on an individual basis to enhance therapeutic response and minimize toxicity. Although a great deal of work remains to fully characterize the limitations and advantages of this technique, our results suggest that DOS is a promising method for evaluating breast cancer and may be applicable to other tumor types.

Acknowledgments

This work was made possible in part by access to National Institutes of Health Centers: the Laser Microbeam and Medical Program (P41 RR-01192) and the Chao Family Comprehensive Cancer Center (CA-62203). Support was also provided by the California Breast Cancer Research Program and the Avon Foundation. DBJ acknowledges funding by the National Institutes of Health Medical Scientist Training Program and AEC acknowledges support from the U.S. Army Medical Research and Material Command (No. DAMD17-98-1-8186). Beckman Laser Institute programmatic support is provided by the AFOSR and the Beckman Foundation. Finally, the authors wish to thank those who generously volunteered for these studies.

References

1. R. W. Carlson and A. M. Favret, ''Multidisciplinary management of locally advanced breast cancer,'' *Breast J.* **5**, 303–307 (1999).
2. B. Fisher, J. Bryant, N. Wolmark, E. Mamounas, A. Brown, E. R. Fisher, D. L. Wickerham, M. Begovic, A. DeCillis, A. Robidoux, R. G. Margolese, A. B. Cruz, Jr., J. L. Hoehn, A. W. Lees, N. V. Dimitrov, and H. D. Bear, ''Effect of preoperative chemotherapy on the outcome of women with operable breast cancer,'' *J. Clin. Oncol.* **16**, 2672–2685 (1998).
3. H. M. Kuerer, A. A. Sahin, K. K. Hunt, L. A. Newman, T. M. Breslin, F. C. Ames, M. I. Ross, A. U. Buzdar, G. N. Hortobagyi, and S. E. Singletary, ''Incidence and impact of documented eradication of breast cancer axillary lymph node metastases before surgery in patients treated with neoadjuvant chemotherapy,'' *Ann. Surg.* **230**, 72–78 (1999).
4. G. Vlastos, N. Q. Mirza, J. T. Lenert, K. K. Hunt, F. C. Ames, B. W. Feig, M. I. Ross, A. U. Buzdar, and S. E. Singletary, ''The feasibility of minimally invasive surgery for stage IIA, IIB, and IIIA breast carcinoma patients after tumor downstaging with induction chemotherapy,'' *Cancer* **88**, 1417–1424 (2000).
5. P. Chollet, S. Charrier, E. Brain, H. Cure, I. van Praagh, V. Feillel, M. de Latour, J. Dauplat, J. L. Misset, and J. P. Ferriere, ''Clinical and pathological response to primary chemotherapy in operable breast cancer,'' *Eur. J. Cancer* **33**, 862–866 (1997).
6. G. Hortobagyi, ''Adjuvant therapy for breast cancer,'' *Ann. Rev. Med.* **51**, 377–392 (2000).
7. M. A. Helvie, L. K. Joynt, R. L. Cody, L. J. Pierce, D. D. Adler, and S. D. Merajver, ''Locally advanced breast carcinoma: accuracy of mammography versus clinical examination in the prediction of residual disease after chemotherapy,'' *Radiology* **198**, 327–332 (1996).
8. M. C. Segel, D. D. Paulus, and G. N. Hortobagyi, ''Advanced primary breast cancer: assessment at mammography of response to induction chemotherapy,'' *Radiology* **169**, 49–54 (1988).
9. M. R. Machiavelli, A. O. Romero, J. E. Perez, J. A. Lacava, M. E. Dominguez, R. Rodriguez, M. R. Barbieri, L. A. Romero Acuna, J. M. Romero Acuna, M. J. Langhi, S. Amato, E. H. Ortiz, C. T. Vallejo, and B. A. Leone, ''Prognostic significance of pathological response of primary tumor and metastatic axillary lymph nodes after neoadjuvant chemotherapy for locally advanced breast carcinoma,'' *Cancer J. Sci. Am.* **4**, 125–131 (1998).
10. E. C. Moskovic, J. L. Mansi, D. M. King, C. R. Murch, and I. E. Smith, ''Mammography in the assessment of response to medical treatment of large primary breast cancer,'' *Clin. Radiol.* **47**, 339–344 (1993).
11. S. Huber, M. Wagner, I. Zuna, M. Medl, H. Czembirek, and S. Delorme, ''Locally advanced breast carcinoma: evaluation of mammography in the prediction of residual disease after induction chemotherapy,'' *Anticancer Res.* **20**, 553–558 (2000).
12. L. D. Feldman, G. N. Hortobagyi, A. U. Buzdar, F. C. Ames, and G. R. Blumenschein, ''Pathological assessent of response to induction

chemotherapy in breast cancer,'' *Cancer Res.* **46**, 2578–2581 (1986).
13. S. J. Vinnicombe, A. D. MacVicar, R. L. Guy, J. P. Sloane, T. J. Powles, G. Knee, and J. E. Husband, ''Primary breast cancer: mammographic changes after neoadjuvant chemotherapy, with pathologic correlation,'' *Radiology* **198**, 333–340 (1996).
14. T. J. Hieken, J. Harrison, J. Herreros, and J. M. Velasco, ''Correlating sonography, mammography, and pathology in the assessment of breast cancer size,'' *Am. J. Surg.* **182**, 351–354 (2001).
15. R. P. Kedar, D. O. Cosgrove, I. E. Smith, J. L. Mansi, and J. C. Bamber, ''Breast carcinoma: measurement of tumor response to primary medical therapy with color Doppler flow imaging,'' *Radiology* **190**, 825–830 (1994).
16. G. C. R. Rizzatto, ''Breast ultrasound and new technologies,'' *Eur. J. Radiol.* **27**, S242–S249 (1998).
17. D. C. Abraham, R. C. Jones, S. E. Jones, J. H. Cheek, G. N. Peters, S. M. Knox, M. D. Grant, D. W. Hampe, D. A. Savino, and S. E. Harms, ''Evaluation of neoadjuvant chemotherapeutic response of locally advanced breast cancer by magnetic resonance imaging,'' *Cancer* **78**, 91–100 (1996).
18. C. Balu-Maestro, C. Chapellier, A. Bleuse, I. Chanalet, C. Chauvel, and R. Largillier, ''Imaging in evaluation of response to neoadjuvant breast cancer treatment benefits of MRI,'' *Breast Cancer Res. Treat* **72**, 145–152 (2002).
19. P. J. Drew, M. J. Kerin, T. Mahapatra, C. Malone, J. R. Monson, L. W. Turnbull, and J. N. Fox, ''Evaluation of response to neoadjuvant chemoradiotherapy for locally advanced breast cancer with dynamic contrast-enhanced MRI of the breast,'' *Eur. J. Surg. Oncol.* **27**, 617–620 (2001).
20. R. Gilles, J. M. Guinebretiere, C. Toussaint, M. Spielman, M. Rietjens, J. Y. Petit, G. Contesso, J. Masselot, and D. Vanel, ''Locally advanced breast cancer: contrast-enhanced subtraction MR imaging of response to preoperative chemotherapy,'' *Radiology* **191**, 633–638 (1994).
21. D. A. Mankoff, L. K. Dunnwald, J. R. Gralow, G. K. Ellis, M. J. Drucker, and R. B. Livingston, ''Monitoring the response of patients with locally advanced breast carcinoma to neoadjuvant chemotherapy using sestamibi scintimammography,'' *Cancer* **85**, 2410–2423 (1999).
22. Y. Takamura, Y. Miyoshi, T. Taguchi, and S. Noguchi, ''Prediction of chemotherapeutic response by technetium-99m-MIBI scintigraphy in breast carcinoma patients,'' *Cancer* **92**, 232–239 (2001).
23. M. Schelling, N. Avril, J. Nahrig, W. Kuhn, W. Romer, D. Sattler, M. Werner, J. Dose, F. Janicke, H. Graeff, and M. Schwaiger, ''Positron emission tomography using [^{18}F]fluorodeoxyglucose for monitoring primary chemotherapy in breast cancer,'' *J. Clin. Oncol.* **18**, 1689–1695 (2000).
24. I. C. Smith, A. E. Welch, A. W. Hutcheon, I. D. Miller, S. Payne, F. Chilcott, S. Waikar, T. Whitaker, A. K. Ah-See, O. Eremin, S. D. Heys, F. J. Gilbert, and P. F. Sharp, ''Positron emission tomography using [^{18}F] fluorodeoxy-D-glucose to predict the pathologic response of breast cancer to primary chemotherapy,'' *J. Clin. Oncol.* **18**, 1676–1688 (2000).
25. W. A. Weber, M. Schwaiger, and N. Avril, ''Quantitative assessment of tumor metabolism using FDG-PET imaging,'' *Nucl. Med. Biol.* **27**, 683–687 (2000).
26. R. Tiling, R. Linke, M. Untch, A. Richter, S. Fieber, K. Brinkbaumer, K. Tatsch, and K. Hahn, ''F-18-FDG PET and Tc-99m-sestamibi scintimammography for monitoring breast cancer response to neoadjuvant chemotherapy: a comparative study,'' *Eur. J. Nucl. Med.* **28**, 711–720 (2001).
27. D. J. Hawrysz and E. M. Sevick-Muraca, ''Developments toward diagnostic breast cancer imaging using near-infrared optical measurements and fluorescent contrast agents,'' *Neoplasia* **2**, 388–417 (2000).
28. V. Ntziachristos, A. G. Yodh, M. Schnall, and B. Chance, ''Concurrent MRI and diffuse optical tomography of breast after indocyanine green enhancement,'' *Proc. Natl. Acad. Sci. U.S.A.* **97**, 2767–2772 (2000).
29. S. Fantini, S. A. Walker, M. A. Franceschini, M. Kaschke, P. M. Schlag, and K. T. Moesta, ''Assessment of the size, position, and optical properties of breast tumors in vivo by noninvasive optical methods,'' *Appl. Opt.* **37**, 1982–1989 (1998).
30. H. Jiang, N. V. Iftimia, Y. Xu, J. A. Eggert, L. L. Fajardo, and K. L. Klove, ''Near-infrared optical imaging of the breast with model-based reconstruction,'' *Acad. Radiol.* **9**, 186–194 (2002).
31. F. Bevilacqua, A. J. Berger, A. E. Cerussi, D. Jakubowski, and B. J. Tromberg, ''Broadband absorption spectroscopy in turbid media by combined frequency-domain and steady-state methods,'' *Appl. Opt.* **39**, 6498–6507 (2000).
32. B. J. Tromberg, N. Shah, R. Lanning, A. Cerussi, J. Espinoza, T. Pham, L. Svaasand, and J. Butler, ''Non-invasive in vivo characterization of breast tumors using photon migration spectroscopy,'' *Neoplasia* **2**, 26–40 (2000).
33. G. Zonios, L. T. Perelman, V. M. Backman, R. Manoharan, M. Fitzmaurice, J. Van Dam, and M. S. Feld, ''Diffuse reflectance spectroscopy of human adenomatous colon polyps in vivo,'' *Appl. Opt.* **38**, 6628–6637 (1999).
34. A. Cerussi, A. Berger, F. Bevilacqua, N. Shah, D. Jakubowski, J. Butler, R. Holcombe, and B. Tromberg, ''Sources of absorption and scattering contrast for near-infrared optical mammography,'' *Acad. Radiol.* **8**, 211–218 (2001).
35. N. Shah, A. Cerussi, C. Eker, J. Espinoza, J. Butler, J. Fishkin, R. Hornung, and B. Tromberg, ''Noninvasive functional optical spectroscopy of human breast tissue,'' *Proc. Natl. Acad. Sci. U.S.A.* **98**, 4420–4425 (2001).
36. T. H. Pham, O. Coquoz, J. B. Fishkin, E. Anderson, and B. J. Tromberg, ''Broad bandwidth frequency domain instrument for quantitative tissue optical spectroscopy,'' *Rev. Sci. Instrum.* **71**, 2500–2513 (2000).
37. A. Ishimaru, *Wave Propagation and Scattering in Random Media*, Academic Press, New York (1978).
38. R. C. Haskell, L. O. Svaasand, Tsong-Tseh Tsay, Ti-Chen Feng, M. S. McAdams, and B. J. Tromberg, ''Boundary conditions for the diffusion equation in radiative transfer,'' *J. Opt. Soc. Am. A* **11**, 2727–2741 (1994).
39. B. J. Tromberg, R. C. Haskell, S. J. Madsen, and L. O. Svaasand, ''Characterization of tissue optical properties using photon density waves,'' *Comments Mol. Cell. Biophys.* **8**, 359–386 (1995).
40. A. Kienle and M. S. Patterson, ''Improved solutions of the steady-state and the time-resolved diffusion equations for reflectance from a semi-infinite turbid medium,'' *J. Opt. Soc. Am. A* **14**, 246–254 (1997).
41. B. J. Tromberg, L. O. Svaasand, T. T. Tsay, and R. C. Haskell, ''Properties of photon density waves in multiple-scattering media,'' *Appl. Opt.* **32**, 607–616 (1993).
42. J. B. Fishkin, O. Coquoz, E. R. Anderson, M. Brenner, and B. J. Tromberg, ''Frequency-domain photon migration measurements of normal and malignant tissue optical properties in a human subject,'' *Appl. Opt.* **36**, 10–20 (1997).
43. N. R. Jagannathan, M. Singh, V. Govindaraju, P. Raghunathan, O. Coshic, P. K. Julka, and G. K. Rath, ''Volume localized in vivo proton MR spectroscopy of breast carcinoma: variation of water-fat ratio in patients receiving chemotherapy,'' *NMR Biomed.* **11**, 414–422 (1998).
44. A. Makris, T. J. Powles, S. Kakolyris, M. Dowsett, S. E. Ashley, and A. L. Harris, ''Reduction in angiogenesis after neoadjuvant chemoendocrine therapy in patients with operable breast carcinoma,'' *Cancer* **85**, 1996–2000 (1999).
45. G. Gasparini, E. Biganzoli, E. Bonoldi, A. Morabito, M. Fanelli, and P. Boracchi, ''Angiogenesis sustains tumor dormancy in patients with breast cancer treated with adjuvant chemotherapy,'' *Breast Cancer Res. Treat* **65**, 71–75 (2001).